

25 July, 1998; To appear in ApJ (Main Journal)

## Flash ionization of the partially ionized wind of the progenitor of SN 1987A.

Peter Lundqvist<sup>1</sup>

### ABSTRACT

The H II region created by the progenitor of SN 1987A was further heated and ionized by the supernova flash. Prior to the flash, the temperature of the gas was  $\sim 4000 - 5000$  K, and helium was neutral, while the post-flash temperature was only slightly less than  $\sim 10^5$  K, with the gas being ionized to helium-like ionization stages of C, N and O. We have followed the slow post-flash cooling and recombination of the gas, as well as its line emission, and find that the strongest lines should be N V  $\lambda 1240$  and O VI  $\lambda 1034$ . Both these lines are good probes for the density of the gas, and suitable instruments to detect the lines are STIS on *HST* and *FUSE*, respectively. Other lines which may be detectable are N IV]  $\lambda 1486$  and [O III]  $\lambda 5007$ , though they are expected to be substantially weaker. The relative strength of the oxygen lines is found to be a good tracer of the color temperature of the supernova flash. From previous observations, we put limits on the hydrogen density,  $n_{\text{H}}$ , of the H II region. The early N V  $\lambda 1240$  flux measured by *IUE* gives an upper limit which is  $n_{\text{H}} \sim 180 \eta^{-0.40} \text{ cm}^{-3}$ , where  $\eta$  is the filling factor of the gas. The recently reported emission in [O III]  $\lambda 5007$  at 2500 days requires  $n_{\text{H}} = (160 \pm 12) \eta^{-0.19} \text{ cm}^{-3}$ , for a supernova burst similar to that in the 500full1 model of Enzman & Burrows (1992). For the more energetic 500full2 burst the density is  $n_{\text{H}} = (215 \pm 15) \eta^{-0.19} \text{ cm}^{-3}$ . These values are much higher than in models of the X-ray emission from the supernova ( $n_{\text{H}} \sim 75 \text{ cm}^{-3}$ ), and it seems plausible that the observed [O III] emission is produced primarily elsewhere than in the H II region. We also discuss the type of progenitor consistent with the H II region. In particular, it seems unlikely that its spectral type was much earlier than B2 Ia.

*Subject headings:* circumstellar matter — supernovae: individual (SN 1987A) — ultraviolet: ISM — hydrodynamics

---

<sup>1</sup>Stockholm Observatory, SE-133 36 Saltsjöbaden, Sweden; E-mail: peter@astro.su.se.

## 1. Introduction

There is mounting evidence that the ejecta of supernova (SN) 1987A are interacting with a relatively dense ( $\sim 10^2 \text{ cm}^{-3}$ ) circumstellar medium (CSM). This CSM was first identified by Chevalier & Dwarkadas (1995, henceforth CD95) as an H II region created by the supernova progenitor. Chevalier & Dwarkadas based their model on the appearance of X-rays (Beuermann, Brandt, & Pietsch 1994; Gorenstein, Hughes, & Tucker 1994), and reappearance and subsequent evolution of radio emission (Staveley-Smith et al. 1992; Ball et al. 1995; Staveley-Smith et al. 1996). Recently, Sonneborn et al. (1998) and Garnavich, Kirshner, & Challis (1997b) have detected broad ( $\sim 2.0 \times 10^4 \text{ km s}^{-1}$ ) Ly $\alpha$  and H $\alpha$  emission, respectively, using the Space Telescope Imaging Spectrograph (STIS) on the *Hubble Space Telescope* (*HST*), clearly indicative of ejecta/CSM interaction (Michael et al. 1998).

The model of CD95 for the formation of the CSM is related to the interacting-winds model of Blondin & Lundqvist (1993) and Martin & Arnett (1995), though CD95 also include the ionizing radiation from the progenitor. The main difference compared to the earlier models is the existence of a rather dense ( $\sim 10^2 \text{ cm}^{-3}$ ), photoionized red supergiant wind inside the denser swept up shell of red supergiant wind. As in the previous models, a large asymmetry of the density in the red supergiant wind seems necessary for the inner ring observed around the supernova (e.g., Jakobsen et al. 1991) to form. In the following we will refer to the photoionized red supergiant wind as the “H II region”.

The density estimated by CD95 for the H II region was confirmed by Borkowski, Blondin, & McCray (1997) to give a satisfactory emission of X-rays, as well as to give a natural explanation to the presently slow expansion of the radio-emitting region ( $2800 \pm 400 \text{ km s}^{-1}$  on day 3200, Gaensler et al. 1997); while the supernova ejecta may expand almost freely in the blue supergiant wind, they slow down to the observed expansion rate in the dense H II region (CD95).

Further possible support to the model of CD95 is the diffuse [O III] emission inside the inner ring reported by Wang et al. (1998). The level of this emission is close to what Wang et al. claim should come from the H II region in the model of CD95. Here we expand on the modeling of the line emission from this gas. In particular, we focus on the UV emission lines and how they constrain the properties of the H II region. This knowledge has implications for estimates of the type of progenitor and the properties of the blue supergiant wind inside the H II region. Knowing the density structure inside the inner ring helps to predict the ejecta/ring collision, and to constrain the initial velocity of the ejecta.

In §2 we discuss the geometry and density of the H II region, and in §3 the flash ionization of this gas. The line emission from the ionized gas is discussed in §4, and its

implications in §5. We summarize our conclusions in §6.

## 2. Pre-flash properties of the H II region

CD95 discussed a 1-D model for the formation of the presupernova nebula. We have updated this model with recent observations to estimate the density and temperature of the H II region. Our model is then used in §3 to calculate the post-flash evolution of the nebula. For simplicity, we have maintained the 1-D scenario of CD95, though we comment on asphericity effects.

The H II region is bounded in the equatorial plane on its outside by the inner ring. Assuming that the [O I] image in Sonneborn et al. (1998) best displays this boundary (see discussions in Lundqvist & Sonneborn 1998, and Sonneborn et al. 1998), and that the distance to the supernova is 50 kpc, we find that the radius of this boundary is  $R = 5.9 \times 10^{17}$  cm.

The inner edge of the H II region can be estimated from the extent of the observed radio emission when this is revived. On day 1550, Gaensler et al. (1997) measure a radius of  $\sim 0''.63$ . Following Chevalier (1998), we assume that the radio turn-on occurs around 1150 days and that the ejecta then have reached  $\sim 0''.61$ . This corresponds to  $r_{\text{II}} \sim 4.5 \times 10^{17}$  cm, if we again assume 50 kpc for the distance.

With a density of  $\sim 10^2$  cm $^{-3}$  (CD95), the ionization balance in the H II region is nearly in steady state before the supernova flash. If we assume that He/H = 0.2, as derived for the inner ring (Lundqvist et al. 1998), Case B recombination of hydrogen, and use the extent of the H II region found above, we can relate the density of the H II region,  $\rho_{\text{II}}$ , to the number of ionizing photons put out by the progenitor per second,  $\dot{S}$ . If helium is not ionized by the progenitor (see below), we find

$$\rho_{\text{II}} \approx 2.0 \times 10^{-22} \left( \frac{\dot{S} - \dot{S}_{\text{ring}}}{10^{45} \text{ s}^{-1}} \right)^{0.5} \left( \frac{T}{5000 \text{ K}} \right)^{0.4} \text{ g cm}^{-3}, \quad (1)$$

where  $T$  is the gas temperature. We have in Eqn. (1) taken into account that some of the ionizing photons are consumed behind the ionization front in the ring, rather than in the low-density H II region. We have called the rate of consumption of ionizing photons in the ring  $\dot{S}_{\text{ring}}$ . A rough limit on  $\dot{S}_{\text{ring}}$  can be obtained if one assumes that the ionization front is at a distance from the inside of the ring corresponding to optical depth unity at 13.6 eV for neutral gas. For a temperature of 5000 K and a hydrogen density of  $10^4$  cm $^{-3}$  in the ring

this means that  $\dot{S}_{\text{ring}} \sim 3.2 \times 10^{45} \text{ s}^{-1}$ . However, as the newly ionized gas flows away from the ionization front its density decreases, which also decreases the value of  $\dot{S}_{\text{ring}}$  needed to keep the gas ionized. While we postpone a more detailed discussion on this to Mellema & Lundqvist 1998 [henceforth ML98], we note that Eqn. (1) provides an upper limit on  $\rho_{\text{II}}$  if we put  $\dot{S}_{\text{ring}} = 0$ .

It is thought that the progenitor was a B3 Ia star (Rousseau et al. 1978), and such stars have  $\dot{S} \sim 3.7 \times 10^{45} \text{ s}^{-1}$  (Panagia 1973). With  $\text{He/H} = 0.2$  we arrive at a number density of hydrogen

$$n_{\text{H}} \lesssim 68 \left( \frac{\dot{S}}{10^{45} \text{ s}^{-1}} \right)^{0.5} \left( \frac{T}{5000 \text{ K}} \right)^{0.4} \text{ cm}^{-3}. \quad (2)$$

To estimate  $T$  we have run photoionization models using a spectrum of a B3 Ia star, approximated by a diluted blackbody with an effective temperature of 16,100 K and  $\dot{S} = 3.7 \times 10^{45} \text{ s}^{-1}$  (Panagia 1973). Abundances are the same as in the calculations for the inner ring by Lundqvist et al. (1998), i.e.,  $(\text{C}+\text{N}+\text{O})/(\text{H}+\text{He}+\text{Z})$  is  $\approx 0.29$  times the solar ratio of Anders & Grevesse (1989), and  $\text{N/C} = 4.5$  and  $\text{N/O} = 1.0$ . The atomic data are also the same. We find that the temperature in the H II region is in the range  $(4.0 - 4.5) \times 10^3 \text{ K}$ , and that helium is indeed neutral. As there is some uncertainty in the iron abundance of the gas (Borkowski et al. 1997), we have also run a model with a factor of 2 depletion of iron so that  $\text{Fe/H} = 1.4 \times 10^{-5}$ . Fe II cooling then becomes less important, and the temperature is slightly higher,  $(4.5 - 5.0) \times 10^3 \text{ K}$ . It seems clear, however, that  $T$  must be substantially lower than the 8000 K assumed by CD95. This has implications for models of the dynamics of the system (see §5.5). As a typical value for  $T$  we have adopted  $T = 4500 \text{ K}$ . Inserting this into Eqn. (2), along with  $\dot{S} = 3.7 \times 10^{45} \text{ s}^{-1}$ , gives  $n_{\text{H}} \lesssim 125 \text{ cm}^{-3}$ .

The values of  $\dot{S}$  in Panagia (1973) were derived for  $T = 7000 \text{ K}$ . A lower value of  $T$  gives a slightly lower value of  $\dot{S}$ , so a better limit on  $n_{\text{H}}$  in our case is therefore  $n_{\text{H}} \lesssim 118 \text{ cm}^{-3}$ . This limit is somewhat higher than the density used by Borkowski et al. (1997) (150 amu  $\text{cm}^{-3}$ , i.e.,  $n_{\text{H}} \sim 75 \text{ cm}^{-3}$  for  $\text{He/H}=0.20$ ) to obtain good agreement between their modeled X-ray spectra and the data of Hasinger, Aschenbach, & Trümper (1996). We note, however, that we only obtain an upper limit on  $n_{\text{H}}$ , and that the value of Borkowski et al. (1997) should be larger if the X-ray emitting gas is more concentrated to the equatorial plane than in their model. Our limit on  $n_{\text{H}}$ , and the X-ray density are therefore consistent.

Guided by this discussion, we have chosen  $n_{\text{H}} = 120 \text{ cm}^{-3}$  as a standard density for

the H II region in our models in §3, though we have also tested other densities. A higher density could be possible (see Eqn. [2]), if the progenitor was of earlier spectral type than B3 Ia. We note from Panagia (1973) that  $\dot{S}$  increases rapidly with earlier spectral type. The spectrum also gets harder, which results in higher  $T$ . Both these effects permit higher limit on  $n_{\text{H}}$  using Eqn. (2). For example, a B2 Ia produces  $\sim 4.1$  times more ionizing photons than a B3 Ia star, corresponding to a factor of  $\gtrsim 2$  higher limit on  $n_{\text{H}}$ .

Low-density cases are also important to investigate, not just because the X-ray models indicate a low density and the fact that  $\dot{S}_{\text{ring}}$  may be non-negligible, but also because the density in the H II region is expected to decrease with distance away from the equatorial plane. How big this density decrease might be is uncertain, but it is unlikely to be as large as in the external red supergiant wind because the sound speed of the gas in the H II region,  $C_{\text{II}} \sim 7.1 (T/5000 \text{ K})^{0.5} \text{ km s}^{-1}$ , is only marginally lower than the velocity of the inner ring ( $v_r \sim 10.3 \text{ km s}^{-1}$ ; Crotts & Heathcote 1992, Cumming & Lundqvist 1997); overpressure in the equatorial plane of the H II gas will create a transverse flow (Chevalier 1998) of nearly isothermal gas to partially compensate for the lower density in the red supergiant wind toward the poles. It seems plausible that one has to go to rather small polar angles to encounter a density which is a factor of  $\sim 2$  lower than in the equatorial plane (see ML98 for further details).

In our models in §3, the density therefore ranges between  $n_{\text{H}} = 60 - 240 \text{ cm}^{-3}$ . Note that when the gas is fully ionized, the electron density is a factor  $\approx 1.4$  higher than  $n_{\text{H}}$ . The temperature of the gas just prior to the supernova flash was set to 4500 K throughout the H II region. The exact value is not important for our results. While hydrogen is ionized, helium is supposed to be neutral.

### 3. Ionization of the H II region by the supernova

To simulate the ionizing radiation from the supernova outburst, we have used the 500full1 and 500full2 models of Enzman & Burrows (1992). Both these bursts were used by Lundqvist & Fransson (1996; henceforth LF96) to give good fits to the light curves of the narrow UV lines from the ring (Sonneborn et al. 1997), and they appear to be limiting cases to the actual burst of SN 1987A (Blinnikov et al. 1998). The degree of ionization in the H II region is therefore similar to that in the innermost part of the ring in the models of LF96; in the case of 500full1, the dominant ionization stages of C, N and O are C V–VI, N VI and O VI–VII, while 500full2 with its higher number of ionizing photons ( $\sim 2.2 \times 10^{57}$  versus  $\sim 1.0 \times 10^{57}$ ) and peak color temperature ( $\sim 1.4 \times 10^6$  versus  $\sim 1.1 \times 10^6$  K) results in C V–VI, N VI–VII and O VII.

The main difference of the H II region compared to the inner ring is the temperature. While the ring is initially neutral, the ionized hydrogen in the H II region cannot contribute to the heating of the gas. This was also discovered by Lundqvist & Fransson (1991) when they calculated the post-explosion temperature of the preionized freely expanding blue supergiant wind. Thus, instead of having maximum temperatures of  $\sim 1.6 \times 10^5$  and  $\sim 2.0 \times 10^5$  K, as are the temperatures of the inner ring for 500full1 and 500full2, respectively, the H II region is in the case of  $n_{\text{H}} = 120 \text{ cm}^{-3}$  only heated to  $(5.9 - 7.9) \times 10^4$  K and  $(6.5 - 9.2) \times 10^4$  K, respectively, with the temperature increasing from the inner edge of the H II region to the outer. For  $n_{\text{H}} = 60$  [240]  $\text{cm}^{-3}$ , the maximum temperatures are  $\approx 7.3 \times 10^4$  [ $8.1 \times 10^4$ ] K and  $\approx 8.2 \times 10^4$  [ $1.0 \times 10^5$ ] K, for 500full1 and 500full2, respectively.

The low density of the H II region ensures slow cooling and recombination. As a matter of fact, even in models with  $n_{\text{H}} = 240 \text{ cm}^{-3}$ , the temperature decrease is only a few per cent until day 1150, which is when we have assumed that the ejecta reach the H II region. From this epoch, we have included the observed X-ray emission of the ejecta/wind interaction (Hasinger et al. 1996) approximated by,

$$L_{\text{sh}} = 1.36 \times 10^{32} \frac{(t - 1150)}{1850} \exp(-E/440) \text{ ergs s}^{-1} \text{ eV}^{-1}. \quad (3)$$

Here  $E$  is the photon energy in eV and  $t$  the time in days since the explosion. While the X-ray emission is unimportant for the ionization of the ring (Lundqvist et al. 1998), it affects marginally the gas in the H II region. For example, the difference in abundances of N III and O III for models with and without X-rays are of the order a few per cent at the present epoch ( $t \sim 4250$  days), and ions of higher ionization stages are affected even less.

A more important effect of the shock than providing ionizing photons is that its outward propagation decreases the fraction of the H II region that can emit narrow lines. We have assumed that the shock velocity remains constant at  $2800 \text{ km s}^{-1}$  after it has reached the H II region. In the equatorial plane this means that the shock has now ( $t \sim 4250$  days) reached  $\sim 5.25 \times 10^{17} \text{ cm}$ .

If we use the 500full1 burst, the temperature in the unshocked H II region at the present epoch ( $t \sim 4250$  days) is  $\sim (7.0 - 7.5) \times 10^4$  K, regardless of the density, while for 500full2, it is  $\sim (7.7 - 8.2) \times 10^4$  K for  $n_{\text{H}} = 60 \text{ cm}^{-3}$  and  $\sim (8.5 - 9.1) \times 10^4$  K for the higher densities. For all these temperatures, the recombination time for N VI to N V is  $\sim 2 \times 10^4 (n_{\text{H}}/120 \text{ cm}^{-3})^{-1}$  days (see Figure 1 of Lundqvist & Fransson, 1991), which means that only  $\sim (15 - 20) \times (n_{\text{H}}/120 \text{ cm}^{-3})\%$  of N VI has recombined to ionization stage V, or lower. A somewhat larger fraction of oxygen has recombined to the same ionization stages. However, almost no recombination proceeds to ionization stage II of either element

because of fast collisional ionization from stage II to III. This immediately tells us that [O II] and [N II] lines must be observationally unimportant (see also §4). The way the ionization depends on density, and the rather marginal difference in ionization for the two markedly different bursts we have used, shows that the burst spectrum is in general less important for the evolution of the ionization structure than the gas density.

## 4. Line emission

### 4.1. Broad emission lines

Borkowski et al. (1997) showed that the interaction of the H II region with the blast wave should give rise to broad emission lines, especially N V  $\lambda 1240$  and O VI  $\lambda 1034$ . Although the lines are weaker than the broad emission lines from the reverse shock, they will constitute an increasing fraction of the total broad emission with time. The flux from the blast wave scales linearly with the preshock fraction of N and O in ionization stages N I–V,  $f_N$ , and O I–VI,  $f_O$ , respectively. For N V  $\lambda 1240$ , Borkowski et al. adopted  $f_N = 0.08$  and for O VI  $\lambda 1034$  they adopted  $f_O = 0.10$ , considered to be lower limits at  $\sim 10$  years.

The value of  $f_N$  used by Borkowski et al. is similar to what we estimate in §3, assuming the gas is initially only in N VI. Looking more closely at our simulations, we note that  $f_N$  scales nearly linearly with density, as expected. In particular for  $n_H = 120 \text{ cm}^{-3}$ ,  $f_N \sim 0.16$  (0.11) for 500full1 (500full2). The lower value for 500full2 is due to a slightly higher temperature, and because  $\sim 22\%$  of the nitrogen starts out at N VII instead of N VI. The value of  $f_N$  adopted by Borkowski et al. (1997) therefore seems adequate for the density they used. The value we find for  $f_O$  at  $\sim 10$  years is  $\sim 0.44 (n_H/120 \text{ cm}^{-3})^{0.44}$  for 500full1 and  $\sim 0.19 (n_H/120 \text{ cm}^{-3})^{0.83}$  for 500full2, for the range of densities we have tested. This could mean a slightly higher O VI  $\lambda 1034$  flux from the blast wave than in the models by Borkowski et al. (1997).

### 4.2. Narrow emission lines

The slow evolution of the temperature and ionization of the H II region has the interesting effect that the UV lines that once dominated the emission from the inner ring (He II  $\lambda 1640$ , C III]  $\lambda 1909$ , N III]  $\lambda 1750$ , N IV]  $\lambda 1486$ , N V  $\lambda 1240$  and O III]  $\lambda 1663$ ; cf. Sonneborn et al. 1997), could still be emitted by the H II region. This is displayed in Figures 1 (for 500full1) and 2 (for 500full2), where we show calculated fluxes of He II  $\lambda 1640$ , N III]  $\lambda 1750$ , N IV]  $\lambda 1486$ , N V  $\lambda 1240$  and O III]  $\lambda 1663$  for various densities. In the panels

showing N V  $\lambda 1240$  we have included the observations of Sonneborn et al. (1997) since these are used in §5.3 to put limits on  $n_{\text{H}}$ . The *International Ultraviolet Explorer (IUE)* observations of the other lines are too close to the noise level (which is of the order of, or slightly less than  $10^{-13}$  ergs  $\text{s}^{-1}$   $\text{cm}^{-2}$  for the dereddened fluxes; cf. LF96) to be useful for our analysis here. In the figures, we have also included the important lines [O III]  $\lambda 5007$  and O VI  $\lambda 1034$ .

Figures 1 and 2 are for two cases: one where we have taken into account the decrease of the volume of the unshocked H II region with time, and another where this decrease has not been included. The latter could be more realistic if the H II region is not spherically symmetric, but instead bulges out to large radii for small polar angles.

If the density of the H II region varies strongly with polar angle, a combination of models with different densities should be more realistic. The models in Figures 1 and 2 could be used for such an analysis, if the fluxes are rescaled according to the expected volumes of the different density components. The fluxes of all lines, except O VI  $\lambda 1034$ , are extremely density-sensitive, which implies that the emission in a multi-density environment will be heavily weighted toward the component with the highest density. Presumably, such a component would reside close to the equatorial plane.

Figures 1 and 2 show the same general behavior of the light curves, except for the O VI line, which decays much faster in the 500full1 case. This is a result of the slightly higher initial ionization of oxygen in the 500full2 case. This, in combination with an also slightly higher temperature in the case of 500full2, makes recombination to O III proceed somewhat slower than for 500full1. To display this more clearly, we show in Figure 3 relative line fluxes at 4250 days, as functions of  $n_{\text{H}}$ . The reference line is N V  $\lambda 1240$ .

As described in Figure 3, the displayed models are for four cases. From these models, it is obvious that while the absolute fluxes of the lines differ markedly depending on whether the full, or reduced size of the H II region is included (see Figures 1 and 2), the *ratios* of the lines are insensitive to the size of the emitting region (see Figure 3). The ratios are, however, sensitive to the burst spectrum. In particular, the strengths of the oxygen lines relative to N V  $\lambda 1240$  at 4250 days differ strongly between the 500full1 and 500full2 cases, and there is also a small difference for the He II  $\lambda 1640$ /N V  $\lambda 1240$  ratio.

We caution that Figures 1–3 display fluxes for the multiplets of the lines. In particular, the N V and O VI lines have two components, N V  $\lambda\lambda 1238.82, 1242.80$  and O VI  $\lambda\lambda 1031.93, 1037.62$ , with the shortward components being twice as bright as the longward. The separation of the components corresponds to  $\approx 9.62 \times 10^2$   $\text{km s}^{-1}$  and  $\approx 1.65 \times 10^3$   $\text{km s}^{-1}$ , respectively. For N V  $\lambda 1240$ , the separation of its components should be large enough not

to blend in STIS spectra.

The lines from the H II region are intrinsically narrow. In the ring plane, the velocity of the gas is expected to be lower than for the ring itself (see ML98). It is in fact likely that thermal broadening of the lines are comparable to the velocity broadening, especially for the He II line, which has a thermal broadening of  $\sim 18 \text{ km s}^{-1}$ . In any case, the lines are significantly narrower than the emission from the hot spot or the ejecta/H II region interaction, and should in STIS spectra really trace the spatial extent of the emission.

## 5. Discussion

### 5.1. Density from existing observations

Figures 1 and 2 show that the line emission from the H II region is sensitive to gas density. In particular, this is true for lines from ions of ionization stages III and IV. It is therefore interesting that Wang et al. (1998) have reported a detection of diffuse [O III]  $\lambda 5007$  emission from the projected region inside the inner ring. The flux at 2500 days was  $f_{[\text{O III}]} = (0.9 \pm 0.3) \times 10^{-14} \text{ ergs s}^{-1} \text{ cm}^{-2}$ . We have included their observation in Figures 1, 2 and 4, where Figure 4 shows calculated [O III]  $\lambda 5007$  fluxes at 2500 days as functions of  $n_{\text{H}}$  for the same models as in Figure 3. It is evident that the [O III] flux is extremely sensitive to density (roughly as  $f_{[\text{O III}]} \propto n_{\text{H}}^{5.4}$ ), but that it is also somewhat sensitive to the burst spectrum. If we include the decrease of the H II region due to the shock propagation, the calculated [O III] flux agrees with the observed when  $n_{\text{H}} = (160 \pm 12) \eta^{-0.19} \text{ cm}^{-3}$  for 500full1, and  $n_{\text{H}} = (215 \pm 15) \eta^{-0.19} \text{ cm}^{-3}$  for 500full2, where  $\eta$  is the filling factor of the gas. Because our models are for spherical symmetry (cf. above), a low value of  $\eta$  would apply if the gas is concentrated to the equatorial plane.

The values we find for  $n_{\text{H}}$  from [O III]  $\lambda 5007$  are slightly higher than that of Wang et al. (1998). This is not surprising since Wang et al. only studied the 500full1 case, and did not include the decrease of the H II region due to the shock propagation. In both our study and that of Wang et al., the estimated densities are upper limits. This is not just because  $\eta$  could be less than unity, but also because part of the diffuse [O III] emission could be produced elsewhere than in the H II region, and that it is only when seen in projection that the emission appears to come from inside the inner ring. (Note that Wang et al. only detect and measure emission from inside the ring.)

Our upper limits on  $n_{\text{H}}$  from the [O III] line may seem compatible with the estimated density from X-ray models of the supernova (Borkowski et al. 1997),  $n_{\text{H}} \sim 75 \text{ cm}^{-3}$  (for He/H = 0.20). However, the factor of  $\gtrsim 2$  difference between the X-ray and [O III] densities

is not so easy to understand. A possible explanation could be that the [O III] emission probes gas further out in the H II region than that at the shock front, and that the density further out is higher. A problem with this interpretation is, however, that the observed [O III] emission is diffuse and not concentrated toward the ring (Wang et al. 1998). Another possibility could be that the spectrum of the burst was softer than in 500full1. This would give a lower value of  $n_{\text{H}}$  in the [O III] models. Again, this is rather unlikely because this would contradict the finding of LF96 that the burst spectrum should be at least as hard as 500full1 in order to model the emission from the inner ring (see also §5.3). The successful modeling of the UV emission lines from the ring also rules out that poor atomic data could cause the different densities in X-ray and [O III] models. (The same data were used both here, and by LF96.)

We are therefore left with the possibilities that the observed [O III] emission at 2500 days is primarily formed elsewhere than in the H II region, or that the X-ray models somehow underestimate the density. If the X-ray density ( $n_{\text{H}} \sim 75 \text{ cm}^{-3}$ ) is correct, Figure 4 shows that the expected [O III] flux at 2500 days is of order  $\sim 10^{-16} \text{ ergs s}^{-1} \text{ cm}^{-2}$ . This is far too low to be detected, and the detected [O III] emission can not come from the H II region if the density is this low. Possible sites of contaminating emission could be the outer rings, the walls of the bipolar nebula, and/or the ejecta/H II region interaction region. It should be noted that the observations of Wang et al. were made through [O III] filters which can not discriminate between broad and narrow emission lines.

The X-ray density could be higher than  $n_{\text{H}} \sim 75 \text{ cm}^{-3}$  if the volume of the X-ray emitting gas is smaller than in the model of Borkowski et al. (1997). This could actually be the case since Borkowski et al. assume a rather small value of  $r_{\text{II}}$  compared to ours,  $3.3 \times 10^{17} \text{ cm}$  and  $4.5 \times 10^{17} \text{ cm}$ , respectively. If a smaller X-ray emitting region could allow for a density as high as  $n_{\text{H}} \sim 120 \text{ cm}^{-3}$ , this could be consistent with a B3 Ia nature of the progenitor (see §2). However, even for such a high density, the [O III] flux at 2500 days would only be of order  $\sim 10^{-15} \text{ ergs s}^{-1} \text{ cm}^{-2}$ . So, for this density too, [O III] emission from elsewhere than the H II region is needed to obtain the flux measured by Wang et al. (1998).

Wang et al. (1998) also give an upper limit to the  $\text{H}\alpha$  flux at 2500 days. Assuming a similar spatial distribution of  $\text{H}\alpha$  compared to that of [O III]  $\lambda 5007$ , their  $\text{H}\alpha$  flux is  $f_{\text{H}\alpha} \lesssim 0.6 \times 10^{-14} \text{ ergs s}^{-1} \text{ cm}^{-2}$ . In our most favorable model for  $\text{H}\alpha$  emission, this only corresponds to a limit  $n_{\text{H}} \gtrsim 220 \text{ cm}^{-3}$ .  $\text{H}\alpha$  is thus not a good probe for  $n_{\text{H}}$ .

Finally, we comment on the flux of N V  $\lambda 1240$  measured by the *IUE* at 1600 – 1800 days. Assuming  $E(B-V) = 0.16$ , with  $E(B-V) = 0.10$  from the LMC and  $E(B-V) = 0.06$  from the Galaxy, and using the extinction curves of Savage & Mathis (1979) and Fitzpatrick (1985), the dereddened flux is  $\sim 2.5 \times 10^{-13} \text{ ergs s}^{-1} \text{ cm}^{-2}$ , though there is a large scatter

in the data (see Figs. 1 and 2). Adopting this flux, our simulations put an upper limit on  $n_{\text{H}}$  from N V  $\lambda 1240$ , which is  $n_{\text{H}} \sim 180 \eta^{-0.40} \text{ cm}^{-3}$  for 500full1, and nearly the same for 500full2. This limit is close to what we find for the [O III] flux at 2500 days, which again indicates that the detected [O III] emission does not mainly come from the H II region.

## 5.2. Which lines to observe and what they probe

Obviously, more observations are needed to explain the discrepancy described in §5.1. If we assume that  $\sim 10^{-14} \text{ ergs s}^{-1} \text{ cm}^{-2}$  is a reasonable limit to detect [O III]  $\lambda 5007$  at 4250 days, the density has to be  $\gtrsim 130 - 140 \text{ cm}^{-3}$  for a burst like 500full1 to give rise to detectable [O III] emission. Although, such a density is on the high side compared to X-ray models, it can not be ruled out from our present knowledge.

To probe lower values of  $n_{\text{H}}$  one should focus on the N IV], N V and O VI lines. They have high excitation energies, and are therefore less confused with emission from the low-temperature inner ring than, e.g., [O III]  $\lambda 5007$ , which has had a rather constant temperature of  $\sim 2.5 \times 10^4 \text{ K}$  since  $\sim 1200$  days (Lundqvist et al. 1998).

There is some contamination of N V  $\lambda 1240$  and O VI  $\lambda 1034$  from the shocked gas in the ejecta/wind interaction zone (Borkowski et al. 1997). This diffuse emission is characterized by a range of velocities from a few hundred  $\text{km s}^{-1}$  (in possible hot spots) up to  $\sim 20,000 \text{ km s}^{-1}$  (Sonneborn et al. 1998). To separate out those emissions from the narrow lines from the H II region, it is essential that the spectral resolution is  $\lesssim 100 \text{ km s}^{-1}$ . This is achieved with both the *Far-Ultraviolet Spectroscopic Explorer (FUSE)* for O VI  $\lambda 1034$ , and *HST/STIS* for the rest of the lines.

At a density of  $n_{\text{H}} = 120 \text{ cm}^{-3}$  and for 500full1, the expected fluxes of the O VI, N V and N IV] lines are  $\sim 1 \times 10^{-13}$ ,  $\sim 1 \times 10^{-13}$  and  $\sim 4 \times 10^{-14} \text{ ergs s}^{-1} \text{ cm}^{-2}$ , respectively. Including reddening, which introduces the correction factors  $\sim 0.11$ ,  $\sim 0.17$  and  $\sim 0.24$ , respectively, for  $E(B-V) = 0.16$  (cf. above), and the possibility that  $\eta < 1$ , the lines may still be observable. For 500full2, the fluxes of the O VI and N V lines are similar to those in models using 500full1, whereas N IV] is down by a factor of  $\sim 2$  (cf. Figs. 1 and 2). Lines from ionization stage III will not be observable for any of the bursts, unless the density is higher. However, if it is, these lines will be extremely useful, since, e.g., the O VI/[O III] and O VI/O III] line ratios are sensitive to the burst spectrum. At a density of  $n_{\text{H}} = 75 \text{ cm}^{-3}$ , the prospects of detecting any lines but the O VI and N V lines seem futile.

Although the UV lines are the most useful to observe in order to narrow down the value of  $n_{\text{H}}$ , limits on [O III]  $\lambda 5007$  are certainly useful too. Using STIS at the present

epoch when the [O III] emission from the H II region should be stronger than at 2500 days, means that [O III] can probe lower densities than at 2500 days. As stated above, the [O III] line may also be useful to place limits on the burst spectrum when combined with the O VI line.

### 5.3. Implications for the early UV line emission

LF96 found that a successful modeling of the early UV lines from the inner ring requires that the inner part of the ring be ionized to at least N VI. Obviously, this means that also the H II region should be ionized to N VI, or higher. While this is in accord with our results in §3, there are possible indications from the early UV line emission studied by *IUE* (Sonneborn et al. 1997) that the ionization of the H II region could have been lower.

The *IUE* observations showed that the N V  $\lambda 1240$  flux turned on between 70.2 – 80.6 days, and that N IV]  $\lambda 1486$  turned on a few days later, some time between 80.6 – 85.2 days. That this is just a recombination effect in the ring is not supported by the results of LF96. It is more likely that the early N V  $\lambda 1240$  emission comes from a separate region which has a shorter light travel time than the near side of the ring, and that this gas is devoid of N IV. Possible such sites could be the H II region, or a part of the bipolar nebula.

If the early N V  $\lambda 1240$  emission comes from the H II region, the emitting gas can certainly not be spherically symmetric, since *IUE* would otherwise have detected N V  $\lambda 1240$  much earlier than at 80.6 days. To be consistent with the observations, the part of the H II region possibly emitting N V  $\lambda 1240$  should instead be concentrated toward the ring, with an inner edge of its emission at  $\gtrsim 0.82R$ , assuming that N IV]  $\lambda 1486$  only comes from the inner ring. This radius is not very different from our assumed inner radius of the H II region,  $r_{\text{II}}/R \approx 0.76$ . The small separation in time between the turn-on of N V  $\lambda 1240$  and N IV]  $\lambda 1486$  is therefore not enough to rule out that the  $\sim 10^2 \text{ cm}^{-3}$  gas in H II region could be responsible for the early N V  $\lambda 1240$  emission.

It is, however, difficult to tie such a scenario into our model, especially since we find that nitrogen is ionized to N VI–VII throughout the H II region even for densities substantially higher than  $240 \text{ cm}^{-3}$ , and we have already ruled out such high densities as the general density of the H II region on several grounds (cf. above). A possibility is that the tentative high-density region emitting early N V  $\lambda 1240$  could be similar to the inward protrusion observed by Garnavich, Kirshner, & Challis (1997a) and Sonneborn et al. (1998). If this is correct, the protrusion should be ionized beyond N IV from the outset. Such a protrusion should reveal itself within the next few years as a hot spot on the near

side of the ring. The alternative scenario for the early N V  $\lambda 1240$  emission is that the line forms in the presumably existing bipolar nebula. Again, this gas should not contain any N III or N IV zones giving rise to detectable emission from the outset.

Another possible indication of early N V in the H II region is that resonance scattering in the H II region by N V  $\lambda\lambda 1238.82, 1240.80$  may be necessary to explain the somewhat delayed peak of the N V  $\lambda 1240$  light curve compared to the peak of the other UV lines (Sonneborn et al. 1997). However, skipping the single high data point for N V  $\lambda 1240$  at  $t = 485$  days, LF96 showed that the expected scattering in the bipolar nebula is sufficient to delay the N V  $\lambda 1240$  emission. To check whether the H II region could add additional scattering, we have calculated the column density of N V through the H II region in our models. We find that the column density is too low ( $\lesssim 10^{11} \text{ cm}^{-2}$ ) in all models to cause an optical depth unity in N V  $\lambda\lambda 1238.82, 1240.80$ .

While the column density of the H II region in our spherically symmetric models is low, a larger column density may be obtained along the line of sight to the rear side of the ring if the H II region bulges out far from the equatorial plane. The line of sight to the rear side of the ring could then pass through geometrically thick parts of the H II region on the near side of the nebula which may cause resonance scattering. However, the velocity shift between these two regions will be too large to result in any important resonance scattering. We therefore conclude that neither the early emergence of N V  $\lambda 1240$ , nor its subsequently delayed emission, contradict the idea that the H II region was ionized to at least N VI in the equatorial plane (see §3.). This is also in accord with the idea that the inner side of the inner ring is ionized to N VI (LF96).

#### 5.4. Implications for the progenitor

The value of  $n_{\text{H}}$  for the H II region has implications for the nature of the progenitor through Eqns. (1 & 2). Even with the high value of  $n_{\text{H}}$  we find from the [O III] flux at 2500 days (see §5.1), the number of ionizing photons is

$$\dot{S} \lesssim \dot{S}_{\text{ring}} + 5.5 (10.0) \times 10^{45} \left( \frac{T}{5000 \text{ K}} \right)^{-0.8} \eta^{-0.38} \text{ s}^{-1} \quad (4)$$

for 500full1 (500full2). If  $\eta$  is not  $\ll 1$ , and  $\dot{S}_{\text{ring}}$  is not larger than estimated in §2, a progenitor more powerful than B2 Ia seems to be ruled out. On the other hand, if we take the density from the X-ray modeling to be a lower limit on  $n_{\text{H}}$ , we find  $\dot{S} \gtrsim 1.2 \times 10^{45} (T/5000 \text{ K})^{-0.8} \text{ s}^{-1}$ . This excludes a progenitor much less powerful than a B3

Ia, which has  $\dot{S} \sim 3.7 \times 10^{45} \text{ s}^{-1}$  (Panagia 1973). The most likely range of spectral types of the progenitor therefore appears to be B4 Ia – B2 Ia, assuming a supergiant classification, which is fully consistent with the classification of Rousseau et al. (1978). A caveat is, however, that multidimensional effects could require a lower photoevaporation rate of the inner ring than in the 1-D case (see §5.6), which could push down the “lower limit” of the spectral type to less ionizing than B4 Ia.

### 5.5. Implications for the blue supergiant wind

From our model of the H II region, we can use pressure balance arguments to sketch the structure of the blue supergiant wind interior to the H II region. In a 1-D scenario, pressure balance between the shocked blue supergiant wind and the H II region gives  $\rho_{\text{II}} C_{\text{II}}^2 = 0.88 \rho_b u_b^2$ , where  $\rho_b$  and  $u_b$  are the density and velocity of the freely expanding blue supergiant wind at the termination shock, i.e., at a radius  $r_b$ . The factor 0.88 stems from Weaver et al. (1977; see also CD95 and ML98). The density of the free wind is given by

$$\rho_b \approx 1.0 \times 10^{-25} \left( \frac{\dot{M}_b}{10^{-8} M_{\odot} \text{ yr}^{-1}} \right) \left( \frac{u_b}{500 \text{ km s}^{-1}} \right)^{-1} \left( \frac{r_b}{10^{17} \text{ cm}} \right)^{-2} \text{ g cm}^{-3}, \quad (5)$$

where  $\dot{M}_b$  is the mass loss rate of the blue supergiant wind. From this we find that

$$\dot{M}_b \approx 4.7 \times 10^{-9} \left( \frac{r_b}{10^{17} \text{ cm}} \right)^2 \left( \frac{T}{5000 \text{ K}} \right)^{1.4} \left( \frac{\dot{S} - \dot{S}_{\text{ring}}}{10^{45} \text{ s}} \right)^{0.5} \left( \frac{u_b}{500 \text{ km s}^{-1}} \right)^{-1} M_{\odot} \text{ yr}^{-1}, \quad (6)$$

which should be compared with the maximum value estimated by Chevalier (1998) to be consistent with the fast expansion of nearly undecelerated ejecta,  $\dot{M}_b \lesssim 6.5 \times 10^{-9} (u_b/500 \text{ km s}^{-1}) M_{\odot} \text{ yr}^{-1}$ . Eliminating  $\dot{M}_b$  from these expressions, we find an upper limit on  $r_b$ , which is

$$r_b \lesssim 1.2 \times 10^{17} \left( \frac{u_b}{500 \text{ km s}^{-1}} \right)^2 \left( \frac{T}{5000 \text{ K}} \right)^{-0.7} \left( \frac{\dot{S} - \dot{S}_{\text{ring}}}{10^{45} \text{ s}} \right)^{-0.25} \text{ cm.} \quad (7)$$

If we consider  $u_b = 750 \text{ km s}^{-1}$  an upper limit on wind velocities of B3 Ia stars (e.g., Lamers, Snow, & Lindholm 1995), and use  $T = 4500 \text{ K}$ , we find that  $r_b$  cannot be

larger than  $\sim 1.4 \times 10^{17}$  cm for  $\dot{S} = 3.7 \times 10^{45}$  s $^{-1}$  and  $\dot{S}_{\text{ring}} \ll \dot{S}$ . Because  $r_b$  is only a weak function of  $(\dot{S} - \dot{S}_{\text{ring}})$ ,  $r_b$  could thus be considerably smaller than the  $2.5 \times 10^{17}$  cm assumed by CD95. In a 1-D scenario, the region of hot shocked blue supergiant wind could therefore have a thickness of as much as  $\sim 3 \times 10^{17}$  cm. The near-vacuum of this region would not slow down the supernova ejecta appreciably, and an extremely high initial velocity of the ejecta ( $\gg 4 \times 10^4$  km s $^{-1}$ ; Chevalier 1998) would seem unnecessary. This agrees with explosion models of the supernova which give maximum velocities of the ejecta  $\sim 4 \times 10^4$  km s $^{-1}$  (Imshennik & Nadyozhin 1989; Enzman & Burrows 1992; Blinnikov et al. 1998).

The situation is different in a multidimensional scenario. While  $r_b$  may still be low, the radius of the contact discontinuity will retract in the equatorial plane due to the poleward flow of the shocked blue supergiant wind (Chevalier 1998). However, it should not retract too much to become incompatible with the evolution of the radio emission from the supernova, i.e., if we believe the maximum ejecta velocity is  $\sim 4 \times 10^4$  km s $^{-1}$ . To avoid such a retraction, the pressure in the equatorial plane of the H II region should be lower too, compared to the 1-D case. It may be that the expected poleward gas flow in the H II region (Chevalier 1998) is enough to unload the pressure in the equatorial plane to allow for a radially extended shocked blue supergiant wind. Otherwise, we may have to invoke a lower photoevaporation rate than assumed in §2 to lower the pressure further.

The shapes of the termination shock, and the contact discontinuity between the blue and red supergiant winds, can only be studied in greater detail by means of multidimensional hydrodynamical simulations (Chevalier 1998; ML98). Detecting narrow lines from the H II region, and how they vary in strength with time, would help to constrain the hydrodynamical models and to obtain a more comprehensive picture of the presupernova nebula. This would aid predictions of the ejecta/ring collision.

## 6. Summary

We have calculated the temperature and ionization of the H II region created by the progenitor of SN 1987A. We find that prior to the explosion, the gas was probably cool,  $T \lesssim 5000$  K, and had neutral helium. Using this as input, we have calculated the ionization, temperature and line emission from the gas after it has been further heated and ionized by the radiation accompanying the supernova breakout. The models used for the breakout were 500full1 and 500full2 of Enzman & Burrows (1992). We find that the temperature of the gas stays relative constant at  $\sim (0.6 - 1.0) \times 10^5$  K until the present epoch, and that the X-ray emission from the ejecta/wind interaction is unimportant for the evolution of

temperature and ionization.

The slow recombination to O III for the density inferred from the circumstellar X-rays,  $150 \text{ a.m.u. cm}^{-1}$ , appears to be inconsistent with [O III] observations at  $t = 2500$  days. This argues that the [O III] emission was probably produced elsewhere than in the H II region. This is also indicated by the limit on  $n_{\text{H}}$  we find from the early *IUE* observations of N V  $\lambda 1240$ . Better lines to probe the density of the H II region are instead N V  $\lambda 1240$  and O VI  $\lambda 1034$ . They can be observed using *HST* and *FUSE*, respectively. Another important line is N IV]  $\lambda 1486$ , whereas lines of lower ionization will only show up if the density is a factor of  $\sim 2$  higher than inferred from the X-rays. The fluxes of all lines could start to decline well before day  $\sim 5000$  due to the propagation of the blast wave.

The limits on density we find, together with the expected size of the H II region, put constraints on the nature of Sk -69.202. We estimate that the upper limit on its spectral type is not much earlier than B2 Ia, which is in accord with the classification by Rousseau et al. (1978).

With the most likely inner and outer radii of the H II region in the equatorial plane,  $\sim 4.5 \times 10^{17}$  and  $\sim 5.9 \times 10^{17}$  cm, respectively, we find that a 1-D approximation of the nebula could put the termination shock of the blue supergiant wind as close as  $\lesssim 1.4 \times 10^{17}$  cm to the star. This would mean an extended region of shocked blue supergiant wind, which would ease the fast expansion of the ejecta. How this ties into a multidimensional scenario can only be explored by 2-D hydrodynamical simulations.

The author is grateful to Garrelt Mellema, Lifan Wang, Roger Chevalier, Claes Fransson, Jason Pun and George Sonneborn for discussions, and to Dick McCray for comments on the manuscript. This research was supported by the Swedish Natural Science Research Council, the Anna-Greta and Holger Crafoord Foundation, and the Swedish Board of Space Research.

## REFERENCES

Anders, E., & Grevesse, N. 1989, *Geochimica et Cosmochimica Acta*, 53, 197  
Ball, L., Campbell-Wilson, D., Crawford, D. F., & Turtle, A. J. 1995, *ApJ*, 453, 864  
Beuermann, K., Brandt, S., & Pietsch, W. 1994, *A&A*, 281, L45  
Blinnikov, S. I., Bartunov, O. S., Lundqvist, P., Utrobin, V., Nomoto, K., & Iwamoto, K. 1998, to be submitted to *ApJ*

Blondin, J. M., & Lundqvist, P. 1993, *ApJ*, 405, 337

Borkowski, K., Blondin, J. M., & McCray, R. 1997, *ApJ*, 476, L31

Chevalier, R. A. 1998, in SN 1987A: Ten Years After, eds. M. I Phillips & N. Suntzeff, A.S.P. Conference Series, in press

Chevalier, R. A., & Dwarkadas, V. V. 1995, *ApJ*, 452, L45 (CD95)

Crotts, A. P. S., & Heathcote, S. R. 1991, *Nature*, 350, 514

Cumming, R. J., & Lundqvist, P., 1997, in Advances in Stellar Evolution, ed. R. T. Rood (CUP:Cambridge), p. 297

Ensman, L., & Burrows, A. 1992, *ApJ*, 393, 742

Fitzpatrick, E. L. 1985, *ApJ*, 299, 219

Gaensler, B. M., Manchester, R. N., Staveley-Smith, L., Tzioumis, A. K., Reynolds, J. E, & Kesteven, M. J. 1997, *ApJ*, 479, 845

Garnavich, P. G., Kirshner, R. P., & Challis, P. M. 1997a, *IAU Circ.* 6710

Garnavich, P. G., Kirshner, R. P., & Challis, P. M. 1997b, *IAU Circ.* 6761

Gorenstein, P., Hughes, J. P., & Tucker, W. H. 1994, *ApJ*, 420, L25

Hasinger, G., Aschenbach, B., & Trümper, J. 1996, *A&A*, 312, L9

Imshennik, V. S., & Nadyozhin, D. K. 1989, *Ap. and Space Phys. Rev.*, 8, 1

Jakobsen, P. et al. 1991, *ApJ*, 369, L63

Lamers, H. J. G. L. M., Snow, T. J., & Lindholm, D. M. 1996, *ApJ*, 455, 269

Lundqvist, P., & Fransson, C. 1991, *ApJ*, 380, 575

Lundqvist, P., & Fransson, C. 1996, *ApJ*, 464, 924 (LF96)

Lundqvist, P., & SINS collaboration 1998, in preparation

Lundqvist, P., & Sonneborn, G. 1998, in SN 1987A: Ten Years After, eds. M. Phillips & N. Suntzeff, A.S.P. Conference Series, in press

Martin, C. M., & Arnett, D. A. 1995, *ApJ*, 447, 378

Mellema, G., & Lundqvist, P. 1998, in preparation (ML98)

Michael, E., McCray, R., Borkowski, K. J., Pun, C. S. J., & Sonneborn, G. 1998, *ApJ*, 492, L143

Panagia, N. 1973, *AJ*, 78, 929

Rousseau, J., Martin, N., Prévot, L., Rebeiro, E., Robin, A., & Brunet, J. P. 1978, *A&AS*, 31 243

Savage, B. D., & Mathis, J. 1979, ARA&A, 17, 73

Sonneborn, G., Fransson, C., Lundqvist, P., Cassatella, A., Gilmozzi, R., Kirshner, R. P., Panagia, N., & Wamsteker, W. 1997, ApJ, 477, 848

Sonneborn, G. et al. 1998, ApJ, 492, L139

Staveley-Smith, L. et al. 1992, Nature, 355, 147

Staveley-Smith, L., Manchester, R. N., Tzioumis, A. K., Reynolds, J. E., & Briggs, D. S., in IAU Colloquium 145: Supernovae and supernova remnants, eds. R. McCray & Z. Wang, Cambridge University Press, p. 309

Wang, L., Wheeler, J. C., Kirshner, R. P., Lundqvist, P., Wampler, E. J., Baade, D., Challis, P. M., Chugai, N. N., Filippenko, A. V., Fransson, C., & Garnavich, P. 1998, submitted to ApJ

Weaver, R., McCray, R., Castor, J., Shapiro, P., & Moore, R. 1977, ApJ, 218, 377

Fig. 1.— Calculated light curves for a few important lines emitted by the H II region for three densities:  $n_{\text{H}} = 60, 120$  and  $240 \text{ cm}^{-3}$ . The supernova breakout has been assumed to be similar to that of the 500full1 model of Enzman & Burrows (1992), and the H II region has been approximated by a spherically symmetric shell with an outer radius of  $5.9 \times 10^{17} \text{ cm}$ . In the models marked by solid lines the inner radius of the H II region is held fixed at  $4.5 \times 10^{17} \text{ cm}$ , whereas in the models marked by dashed lines, the increase of the inner radius due to the propagation of the blast wave has been included. The distance to the supernova has been set to 50 kpc, and no reddening has been included. The [O III]  $\lambda 5007$  observation is from Wang et al. (1998), and the N V  $\lambda 1240$  observations are from Sonneborn et al. (1997) assuming  $E(B-V) = 0.16$  (see text).

Fig. 2.— Same as in Fig. 1, but for the 500full2 model of Enzman & Burrows (1992). Note that the N III], O III] and [O III] lines are notably weaker than in Fig. 1.

Fig. 3.— Calculated line ratios, relative to N V  $\lambda 1240$ , for He II  $\lambda 1640$ , N III]  $\lambda 1750$ , N IV]  $\lambda 1486$ , O III]  $\lambda 1663$ , [O III]  $\lambda 5007$  and O VI  $\lambda 1034$  at  $t = 4250$  days. The line ratios are for four cases: the 500full1 burst with a reduced (see Fig. 1) H II region (solid lines), 500full1 with the full H II region (dashed lines), 500full2 with a reduced H II region (long-dashed lines), and 500full2 with the full H II region (dashed-dotted lines). Note that while the absolute fluxes of the lines differ significantly depending on whether the full, or reduced size of the H II region is included (see Figs. 1 and 2), the *ratios* of the lines are insensitive to this. The effect of reddening has not been included.

Fig. 4.— Calculated [O III]  $\lambda 5007$  flux at  $t = 2500$  days as a function of density for the models described in Figure 3. A distance of 50 kpc has been assumed, but no reddening was included. The observed flux is from Wang et al. (1998). Note the strong dependence of the flux on density.

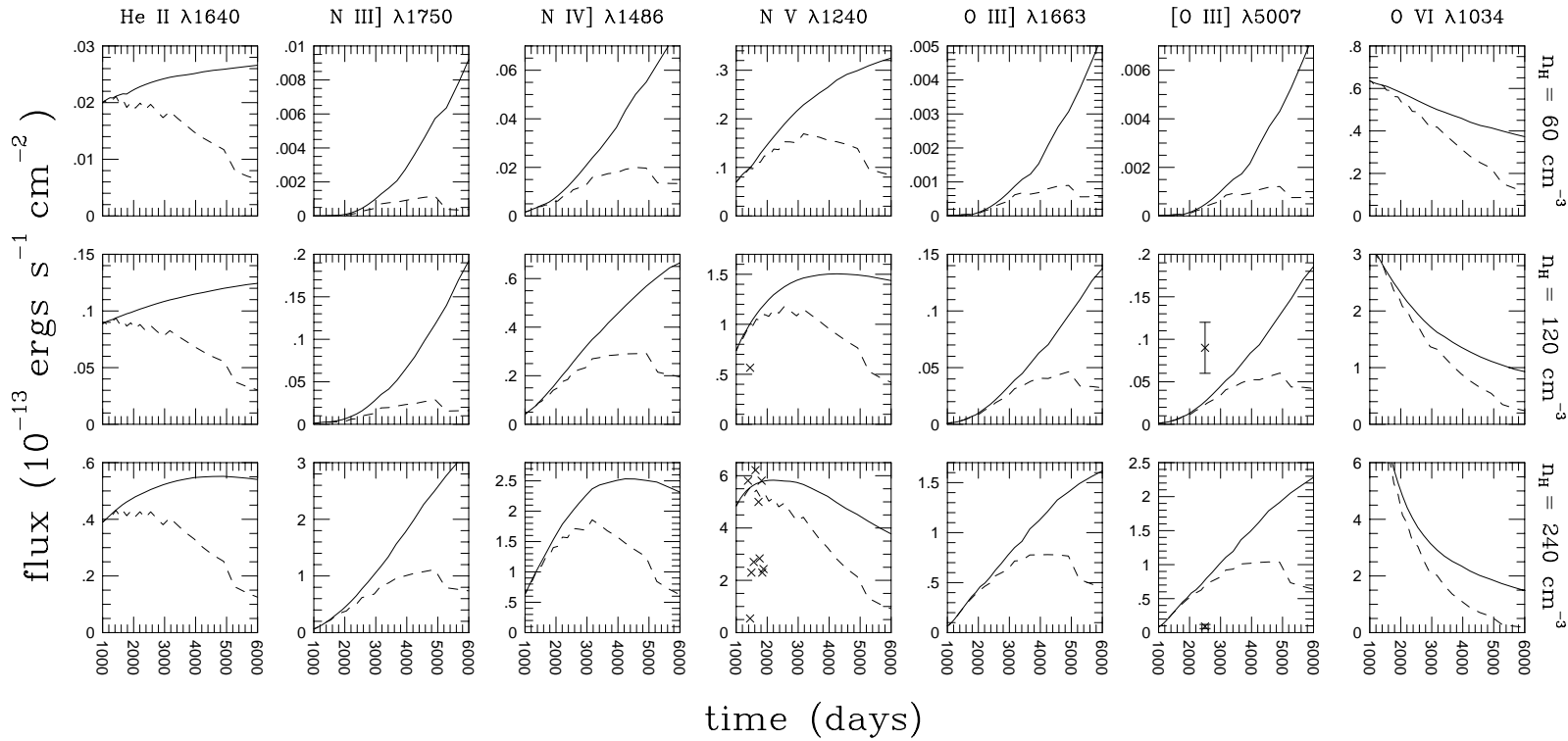


Fig. 1.—

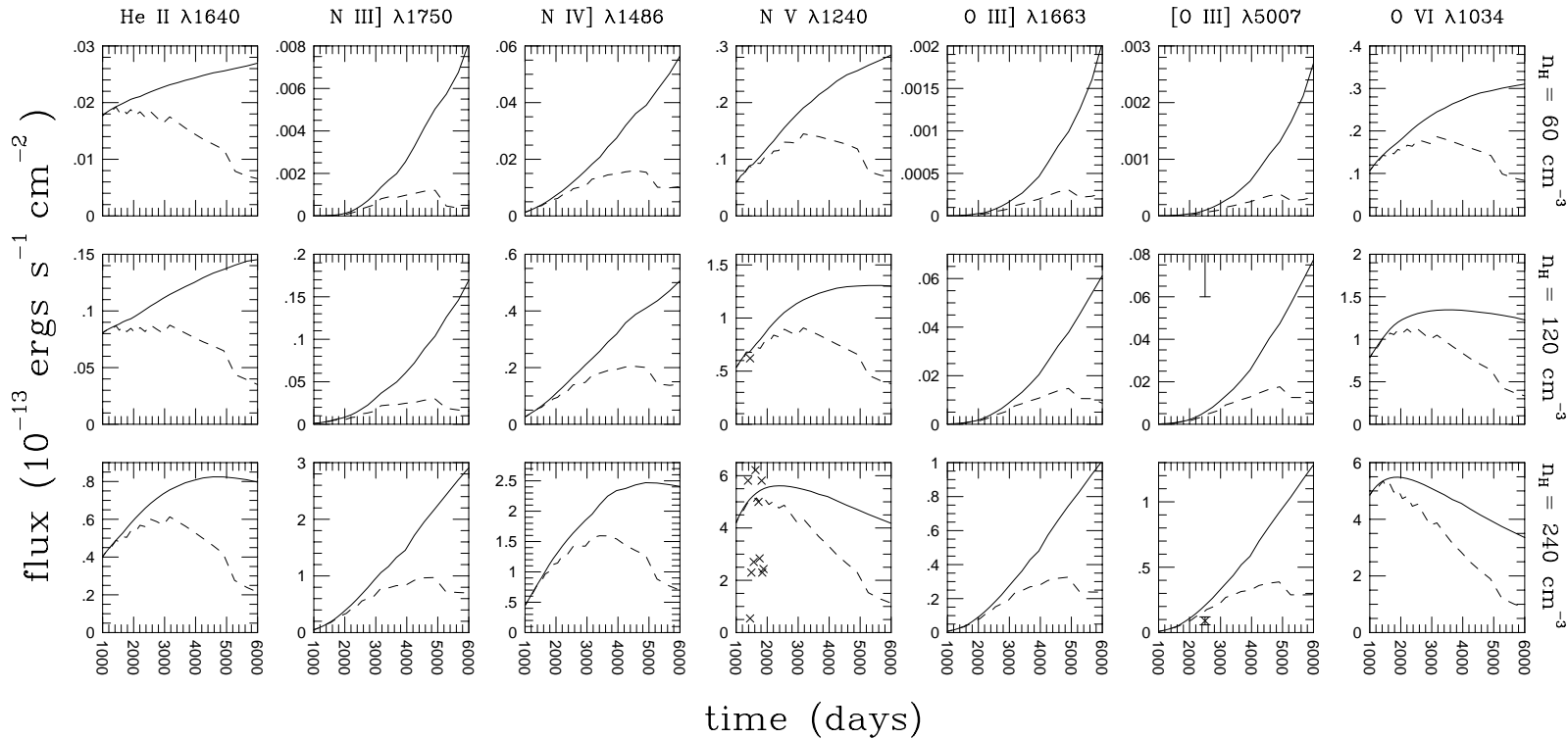


Fig. 2.—

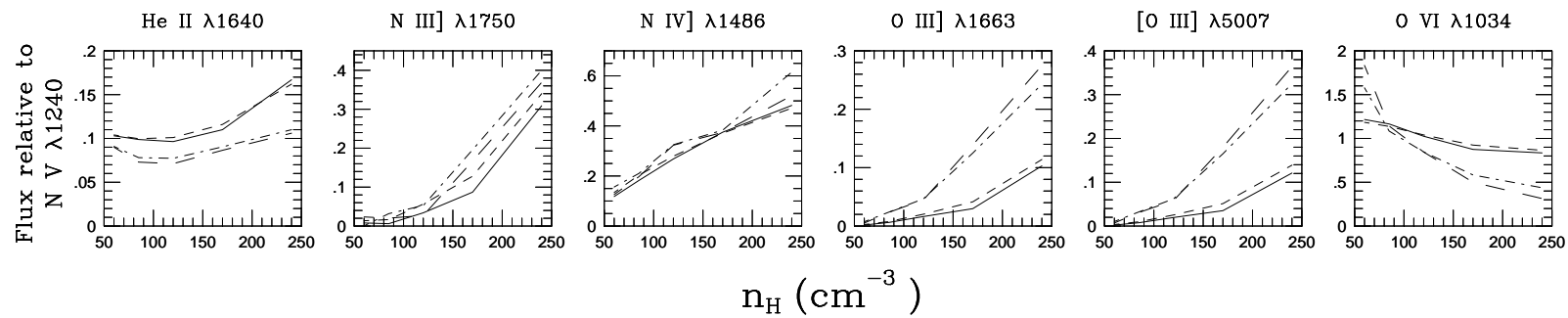


Fig. 3.—

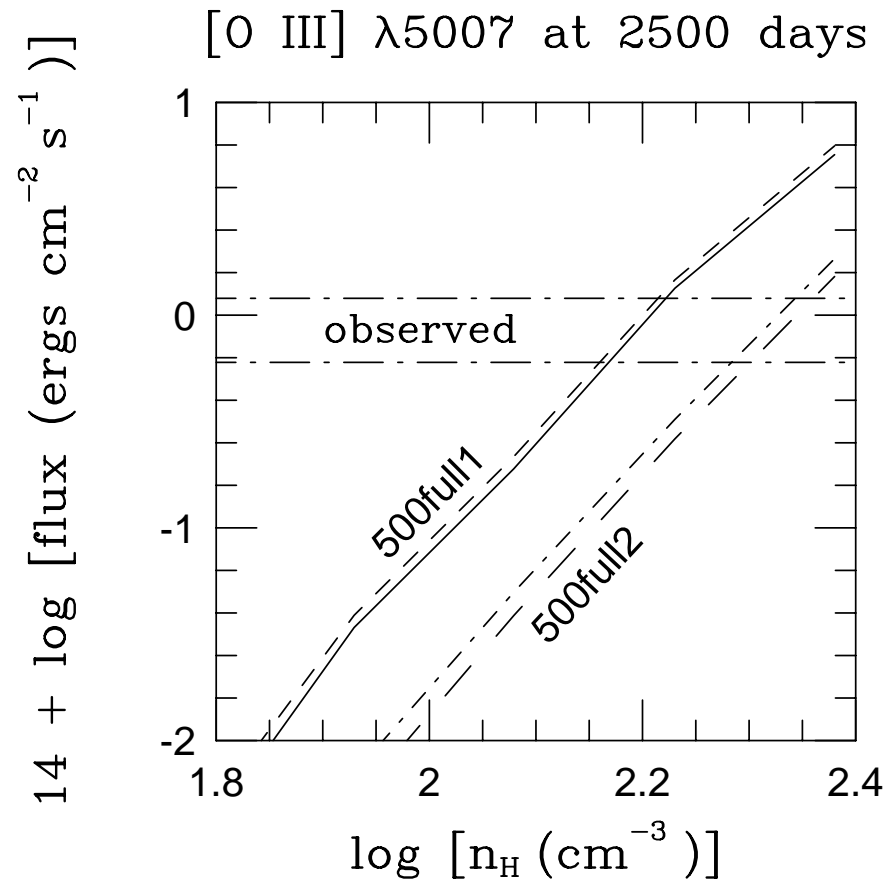


Fig. 4.—